Journal of Alloys and Compounds 509 (2011) 3128–3131

Contents lists available at ScienceDirect

Journal of Alloys and Compounds

journal homepage: www.elsevier.com/locate/jallcom

Synthesis and characterization of $YNbTiO_6:Dy^{3+}$ phosphor

Yurong Shi, Yuhua Wang*, Zhigang Yang

Department of Materials Science, School of Physical Science and Technology, Lanzhou University, No. 222 South Tianshui Road, Lanzhou 730000, PR China

ARTICLE INFO

Article history:
Received 25 July 2010
Received in revised form 3 December 2010
Accepted 3 December 2010
Available online 10 December 2010

Keywords:
Phosphor
$YNbTiO_6:Dy^{3+}$
Luminescence properties
LED

ABSTRACT

A novel yellow phosphor of Dy^{3+} activated $YNbTiO_6$ has been prepared by high temperature solid-state reaction, and its luminescence properties have been investigated. The excitation spectra monitored at 575 nm have several strong peaks from 350 to 480 nm. Under 365 nm excitation, the emission spectra of composition-optimized $(Y_{0.9}Dy_{0.1})NbTiO_6$ phosphor exhibit a dominant peak located at about 575 nm with the Commission Internationale de l'Eclairage (CIE) chromaticity coordinates of (0.385, 0.411). The energy transfer between Dy^{3+} is found to be through exchange interaction.

1. Introduction

Efficacies for commercial phosphor converted light-emitting diodes (LEDs) using blue InGaN LEDs and $Y_3Al_5O_{12}:Ce^{3+}$ garnet-based phosphors are greater than those of the compact fluorescent and linear fluorescent lamps, and can exceed 80 lm/W for 1 W devices [1]. High-efficiency white LEDs are expected to replace the compact fluorescent lamps in the near future [2,3]. However, there are some problems to be solved, such as color changes with input power, low color rendering index due to two-color mixing and low color reproducibility [4]. Considerable efforts which will provide solutions to these problems are going on to obtain novel phosphors.

It is well known that rare-earth-doped oxide phosphors have found to be excellent luminescent materials for their high luminescence efficiency. One of the commonly used lanthanides is Dy^{3+}. In general, Dy^{3+} doped phosphors exhibit several excitation peaks in UV and blue range, and Dy^{3+} doped materials usually have three visible emission peaks including the blue emission at about 480 nm, the yellow emission at about 575 nm and the feeble red emission at about 665 nm, corresponding to $^4F_{9/2}$–$^6H_{15/2}$, $^4F_{9/2}$–$^6H_{13/2}$ and $^4F_{9/2}$–$^6H_{11/2}$ transition, respectively [5–8]. The yellow emission of Dy^{3+} is especially hypersensitive ($\Delta L = 2$, $\Delta J = 2$) to local environment, while its blue emission is not [5–8]. Since the luminescence properties of Dy^{3+} depend on local environment in a given host material, it is of great interest and importance to search materials that give intense emission of Dy^{3+}. Thus, Dy^{3+} doped materials have been intensively studied in recent years, such as $KY_3F_{10}:Dy^{3+}$, $LiLuF_4:Dy^{3+}$ [9], $Gd_3Al_5O_{12}:Dy^{3+}$ [10], $Gd_2(MoO_4)_3:Dy^{3+}$ [11], $SnO_2:Dy^{3+}$ [12], $Ca_3La(VO_4)_3:Dy^{3+}$ [13] and $M_5(PO_4)_3F:Dy^{3+}$ [14].

The desirable factor of $YNbTiO_6$ as host for rare earth ions (RE^{3+}) is that RE^{3+} ions have similar radius and physical–chemical properties with Y^{3+}. When one Y^{3+} is replaced by RE^{3+}, the crystal structure does not change dramatically and also without any charge compensation problems [15]. Recently, $YNbTiO_6$ have been reported to be good host materials for Eu^{3+} phosphor emitting luminescence [16]. However, to the best of our knowledge, the luminescence properties of Dy^{3+}-activated $YNbTiO_6$ phosphor have not been reported yet. In this study, $YNbTiO_6:Dy^{3+}$ phosphor was synthesized and its luminescence properties were investigated.

2. Experimental

The phosphors $(Y_{1-x}Dy_x)NbTiO_6$ ($0 \le x \le 0.17$) were synthesized by a high temperature solid-state reaction method in air. The starting materials of Y_2O_3 (better than 99.99%), Nb_2O_5 (A.R.), TiO_2 (A.R.) and high purity Dy_2O_3 (better than 99.99%) were weighed by appropriate stoichiometric ratio. After being ground and blended thoroughly in an agate mortar, the homogeneous mixtures were fired at 1200, 1300, 1400 °C for 5 h in air, respectively.

The phase purity was determined by using a Rigaku D/MAX-2400 powder X-ray diffractometer (XRD) with Cu Kα radiation ($\lambda = 1.54178$ Å) operating at 40 kV and 60 mA. Both excitation and emission spectra were measured by HORIBA JOBIN YVON Fluorlog-3 spectrofluorometer system. The CIE chromaticity coordinates of all samples were calculated by "ZolixColorConvert 1.0" program (Beijing Zolix Instruments Co., Ltd.). All the luminescence characteristics of the phosphors were carried out under ambient atmosphere.

---

* Corresponding author. Tel.: +86 931 8912772; fax: +86 931 8913554.
E-mail address: wyh@lzu.edu.cn (Y. Wang).

0925-8388/$ – see front matter © 2010 Elsevier B.V. All rights reserved.
doi:10.1016/j.jallcom.2010.12.018

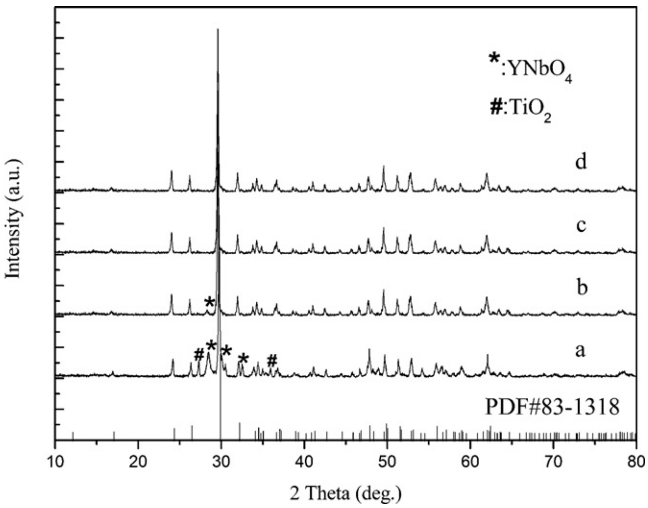

Fig. 1. XRD patterns of $(Y_{1-x}Dy_x)NbTiO_6$ ($0 \leq x \leq 0.17$) samples fired at: (a) $x = 0$, 1200 °C, (b) $x = 0$, 1300 °C, (c) $x = 0$, 1400 °C, and (d) $x = 0.10$, 1400 °C for 5 h in air. The standard XRD pattern of $YNbTiO_6$ is taken from JCPDS card no. 83-1318.

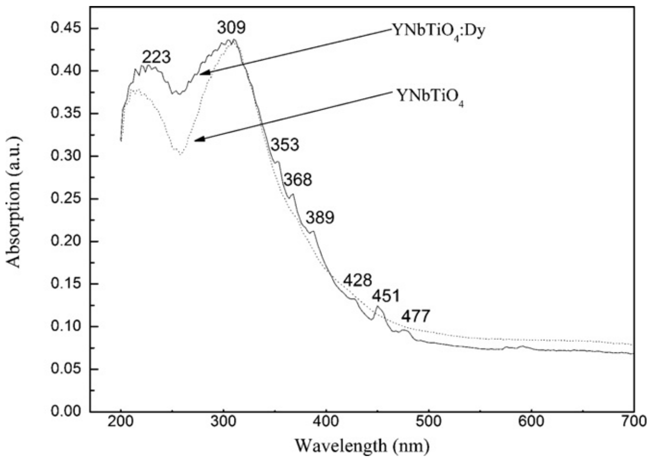

Fig. 2. Absorption spectra of $YNbTiO_6$ and $YNbTiO_6$:Dy^{3+}.

3. Results and discussion

3.1. XRD patterns of synthesized $YNbTiO_6$

Euxenite-type $YNbTiO_6$ is composed of distorted $Nb(Ti)O_6$ octahedral double layers joined together by edge and corner sharing and an YO_8 irregular polyhedron single layer which divides neighboring $Nb(Ti)O_6$ [17]. The XRD patterns of $YNbTiO_6$ and $YNbTiO_6$:$0.1Dy^{3+}$ samples at different annealing temperatures are shown in Fig. 1. With reaction temperatures at 1200 °C for 5 h, the intermediate phase $YNbO_4$ appears, and a very small amount of TiO_2 is also observed, which are confirmed by JCPDS card no. 23-1486 and JCPDS card no. 65-0191, respectively. This indicates that the reaction is incomplete under such temperature. The intensity of impurity phases decrease with the increasing annealing temperature. With the reaction temperature up to 1400 °C, a pure phase of $YNbTiO_6$ is obtained, whose XRD pattern is found to be consistent with that reported in JCPDS card no. 83-1318. Fig. 1 also shows XRD pattern of the $YNbTiO_6$:$0.1Dy^{3+}$ phosphor. No obvious differences are found in the XRD patterns of $YNbTiO_6$ sample and $YNbTiO_6$:$0.1Dy^{3+}$ phosphor. Hence, doping 0.1% Dy^{3+} is not expected to change XRD pattern.

3.2. Photoluminescence properties of $YNbTiO_6$:Dy^{3+} phosphors

Absorption spectra of $YNbTiO_6$ and $YNbTiO_6$:Dy^{3+} samples are shown in Fig. 2. Two broad bands and several small peaks are observed in the absorption spectrum of $YNbTiO_6$:Dy^{3+}. However, the absorption spectrum of pure $YNbTiO_6$ shows only two broad bands. Therefore small peaks at 353, 368, 389, 428, 451, and 477 nm

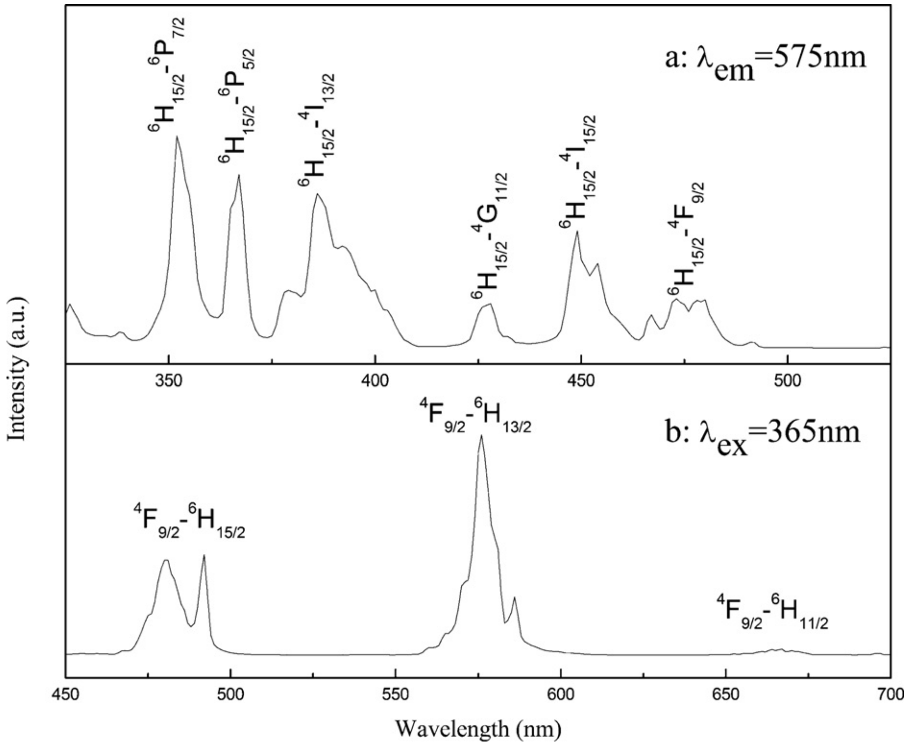

Fig. 3. The excitation (a) and emission (b) spectra of $YNbTiO_6$:$0.1Dy^{3+}$.

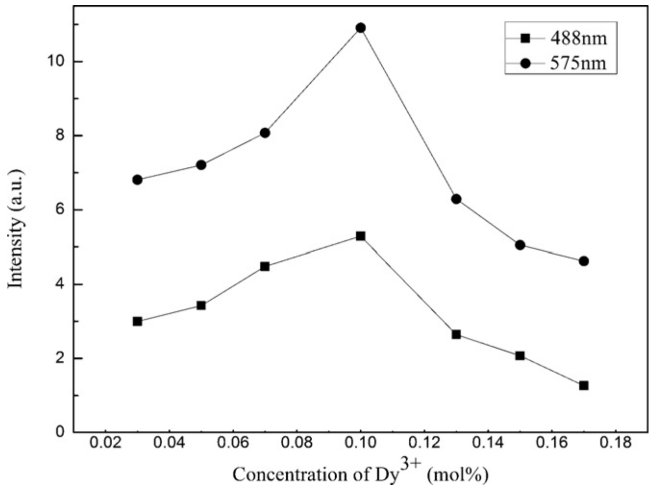

Fig. 4. The effect of Dy^{3+} concentration on the intensity of two emission peaks of $YNbTiO_6$:Dy^{3+}.

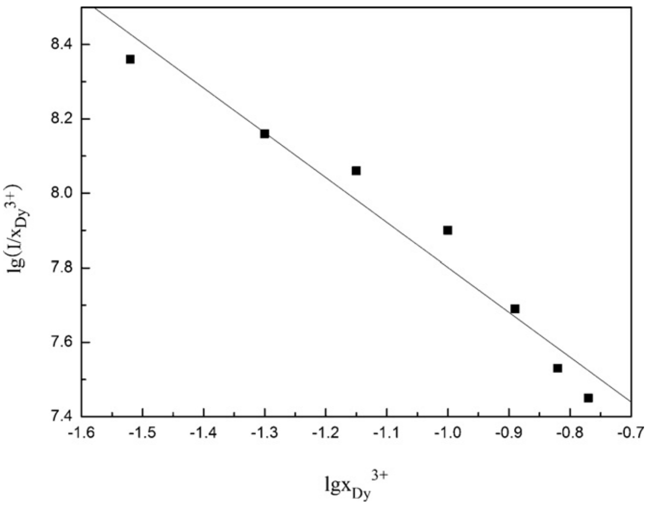

Fig. 5. Log plot for the emission intensity at 575 nm per activator ions as a function of the activator concentration.

must be due to Dy^{3+}, and the absorption bands with maximum at 223 and 309 nm to the host lattice $YNbTiO_6$.

Fig. 3 shows the excitation (a) and emission (b) spectra of the $YNbTiO_6$:$0.1Dy^{3+}$ phosphor. As the profiles of all excitation and emission spectra are similar, only the spectra of $YNbTiO_6$:$0.1Dy^{3+}$ phosphor are given as an example. The emission spectrum of $YNbTiO_6$:$0.1Dy^{3+}$ phosphor shows three groups of peaks centered at about 488, 575, and 660 nm under 365 nm excitation, which originate from the transitions of ${}^4F_{9/2}$–${}^6H_{15/2}$, ${}^4F_{9/2}$–${}^6H_{13/2}$ and ${}^4F_{9/2}$–${}^6H_{11/2}$ of Dy^{3+}, respectively [5–8]. It is worth notice that the two typical emission peaks are split in different ways. The energy level transition of ${}^4F_{9/2}$–${}^6H_{15/2}$ is split into 480 and 492 nm emission peaks and ${}^4F_{9/2}$–${}^6H_{13/2}$ into 575 and 586 nm emission peaks. These splittings are result of the crystal field effects, whose magnitudes are closely related to the strength and symmetry of $YNbTiO_6$ crystal field. It can also be observed from Fig. 3 that yellow emission at about 575 nm is stronger than blue emission at about 488 nm. It is well known that ${}^4F_{9/2}$–${}^6H_{13/2}$ transition of Dy^{3+} belongs to hypersensitive transitions with $\Delta J = 2$. When Dy^{3+} is located at a low-symmetry local site (without an inversion center), this emission transition dominates in emission spectra, otherwise the blue emission is dominant [18]. So it is believed that Dy^{3+} is located at a low symmetry in $YNbTiO_6$:Dy^{3+} phosphor. The excitation spectrum monitored at 575 nm has several strong excitation peaks at 353, 368, 389, 428, 451 and 477 nm which are corresponding to the transitions of Dy^{3+} from the ${}^6H_{15/2}$ ground state to ${}^6P_{7/2}$, ${}^6P_{5/2}$, ${}^4I_{13/2}$, ${}^4G_{11/2}$, ${}^4I_{15/2}$ and ${}^4F_{9/2}$, respectively [19]. The excitation spectrum shows a striking agreement with the absorption spectrum of $YNbTiO_6$:Dy^{3+} phosphor. Besides, peaks located at UV region are stronger than that of blue region which indicates that $YNbTiO_6$:Dy^{3+} phosphor is more suitable for UV LED chip than blue LED chip.

3.3. *Effect of concentration of Dy^{3+} on luminescent properties of $YNbTiO_6$:Dy^{3+} phosphors*

Doping concentration is an important factor influencing the performance of luminescent materials. Herein we determine the optimum concentration. Under the 365 nm excitation, the effect of Dy^{3+} concentration on the intensity of two emission peaks of $YNbTiO_6$:Dy^{3+} is shown in Fig. 4. The effect of two emission peaks influenced by Dy^{3+} concentration is very similar. When Dy^{3+} concentration exceeds 10 mol%, the intensities decrease for both 575 nm and 488 nm emissions. The CIE coordinates of composition-optimized $(Y_{0.9}Dy_{0.1})NbTiO_6$ phosphor is at (0.385, 0.411) under 365 nm excitation. As mentioned above, ${}^4F_{9/2}$–${}^6H_{13/2}$ transition of Dy^{3+} belongs to hypersensitive transitions and the intensity is strongly influenced by the surrounding environment around the Dy^{3+}, while the intensity of 488 nm is less sensitive to the host [8,20,21]. However, the ratio of ${}^4F_{9/2}$–${}^6H_{15/2}$ transition to ${}^4F_{9/2}$–${}^6H_{13/2}$ transition (B/Y) is almost constant over the full range of Dy^{3+} concentration in this host, which indicates that high concentration of Dy^{3+} does not greatly change surrounding environment. This phenomenon is different from Dy^{3+} in other hosts, such as $Ca_8Mg(SiO_4)Cl_2$ [22] and $REAl_3(BO_3)_4$ [23] host. In the case of Dy^{3+}-doped $Ca_8Mg(SiO_4)Cl_2$ and $REAl_3(BO_3)_4$ phosphors, different Dy^{3+} concentration causes different ratio of B/Y.

3.4. *Mechanism of energy transfer in $YNbTiO_6$:Dy^{3+} phosphors*

Energy transfer is generally associated with multipolar interactions, radiation reabsorption, or exchange interaction. Among them, Multipolar interactions are usually prevalent which have several types, such as dipole–dipole (d–d), dipole–quadrupole (d–q), and quadrupole–quadrupole (q–q) interactions. Exchange interaction is generally limited to interactions between RE ions in nearest or next nearest neighbor. If migration is rapid compared to direct transfer, quenching tends to be proportional to quenching-ions concentration [24]. For a better understanding of energy transfer in the host, the relationship of emission intensity and activator concentration is discussed. As the report of Van Uitert and Ozawa, The type of energy transfer can be determined from the change in the emission intensity from the emitting level [24,25]. The emission intensity (I) per activator ion follows the equation:

$$\frac{I}{x} = K[1 + \beta(x)^{\theta/3}]^{-1} \qquad (1)$$

where x is the activator concentration, I/x is the emission intensity (I) per activator concentration (x), and K and β are constants for the same excitation condition for a given host crystal. According to Eq. (1), $\theta = 3$ for the energy transfer among the nearest-neighbor ions, while $\theta = 6$, 8, 10 for d–d, d–q, q–q interactions, respectively. According to Ref. [26], Eq. (1) can simply be rearranged as follows:

$$\ln\left(\frac{I}{x}\right) = K' - \frac{\theta}{3}\ln x (K' = \ln K - \ln\beta) \qquad (2)$$

From the slope of Eq. (2), θ can be obtained. To get the value for Dy^{3+} sites in the host material $YNbTiO_6$, we have used 365 nm to excite the $YNbTiO_6$:Dy^{3+} phosphors, measured the emission intensities (I) of $^4F_{9/2}$–$^6H_{13/2}$ (575 nm) transition and plotted the concentration dependence curves ($\log(I/x) - \log x$) as shown in Fig. 5. From the curves, it can be found that the slope is -1.11, so θ is 3.33 which is approximately equal to 3, which means that the quenching is directly proportional to the ion concentration. The result indicates that the concentration quenching for the Dy^{3+}-site emission centers is caused by exchange interaction in the $YNbTiO_6$:Dy^{3+} phosphor.

4. Conclusions

In summary, Dy^{3+}-activated $YNbTiO_6$ phosphors have been synthesized by a high temperature solid-state reaction method at 1400 °C for 5 h. Their luminescence properties have been investigated. The excitation spectra of the phosphor consist of several sharp peaks due to f–f transition of Dy^{3+}. The emission spectra consist of three emission ranges originated from $^4F_{9/2}$–$^6H_{15/2}$, $^4F_{9/2}$–$^6H_{13/2}$ and $^4F_{9/2}$–$^6H_{11/2}$ transition, respectively, and the intensity of $^4F_{9/2}$–$^6H_{13/2}$ is stronger than that of others. The effect of Dy^{3+} concentration on the emission intensity of $YNbTiO_6$:Dy^{3+} phosphor has also been researched. The results indicate that for both 575 nm and 488 nm emissions the intensities grow with the increasing Dy^{3+} concentration till the maximum value is reached at 10 mol% of Dy^{3+}, and then decrease. The CIE coordinates of composition-optimized $(Y_{0.9}Dy_{0.1})NbTiO_6$ phosphor is at (0.385, 0.411) under 365 nm excitation. The type of energy transfer has been discussed and found to be exchange interaction.

Acknowledgements

This work was supported by the National Science Foundation for Distinguished Young Scholars (No. 50925206), the National Natural Science Foundation of China (No. 10874061) and the Research Fund for the Doctoral Program of Higher Education (No. 200807300010).

References

[1] A.A. Setlur, W.J. Heward, M.E. Hannah, U. Happek, Chem. Mater. 20 (2008) 6277–6283.
[2] T. Fujii, Y. Gao, R. Sharma, E.L. Hu, S.P. DenBaars, S. Nakamura, Appl. Phys. Lett. 84 (2004) 855–857.
[3] Y.X. Qin, S.Y.R. Hui, IEEE Trans. Power Electron. 25 (2010) 507–513.
[4] J.S. Kim, P.E. Jeon, J.C. Choi, H.L. Park, S.I. Mho, G.C. Kim, Appl. Phys. Lett. 82 (2004) 2931–2933.
[5] Y.H. Wang, Y. Wen, F. Zhang, Mater. Res. Bull. 45 (2010) 1614–1617.
[6] R.P. Wei, Z.H. Ju, J.X. Ma, D. Zhang, Z.P. Zang, W.S. Liu, J. Alloys Compd. 486 (2009) L17–L20.
[7] J.P. Zhong, H.B. Liang, B. Han, Z.F. Tian, Q. Su, Y. Tao, Opt. Express 16 (2008) 7508–7515.
[8] C.K. Jayasankar, V. Venkatramu, S. Surendra Babu, P. Babu, J. Alloys Compd. 374 (2004) 22–26.
[9] S. Bigotta, M. Tonelli, E. Cavalli, A. Belletti, J. Lumin. 130 (2010) 13–17.
[10] G.S.R. Raju, H.C. Jung, J.Y. Park, C.M. Kanamadi, B.K. Moon, J.H. Jeong, S. Son, J.H. Kim, J. Alloys Compd. 481 (2009) 730–734.
[11] L.H. Cheng, X.P. Li, J.S. Sun, H.Y. Zhong, Y. Tian, J. Wan, W.L. Lu, Y.F. Zheng, T.T. Yu, L.B. Huang, H.Q. Yu, B.J. Chen, Physica B 405 (2010) 4457–4461.
[12] S.K. Pillai, L.M. Sikhwivhilu, T.K. Hillie, Mater. Chem. Phys. 120 (2010) 619–624.
[13] B.V. Rao, K. Jang, H.S. Lee, S.S. Yi, J.H. Jeong, J. Alloys Compd. 496 (2010) 251–255.
[14] I.M. Nagpure, K.N. Shinde, S.J. Dhoble, A. Kumar, J. Alloys Compd. 481 (2009) 632–638.
[15] R.P. Rao, D.J. Devine, J. Lumin. 87–89 (2000) 1260–1263.
[16] Q. Ma, Y.Y. Zhou, A.Y. Zhang, M.K. Lu, G.J. Zhou, C.Z. Li, Solid State Sci. 11 (2009) 1124–1130.
[17] X. Qi, R. Illingworth, H.G. Gallagher, T.P.J. Han, B. Henderson, J. Cryst. Growth 160 (1996) 111–118.
[18] M. Yu, J. Lin, Z. Wang, J. Fu, S. Wang, H.J. Zhang, Y.C. Han, Chem. Mater. 14 (2002) 2224–2231.
[19] G.B. Kumar, S. Buddhudu, Physica B 403 (2008) 4164–4170.
[20] M. Jayasimhadri, B.V. Ratnam, K. Jang, H.S. Lee, J. Am. Ceram. Soc. 93 (2010) 494–499.
[21] R. Zhang, X. Wang, J. Alloys Compd. 509 (2011) 1197–1200.
[22] Y. Fang, W.D. Zhuang, Y.S. Hu, X.Y. Ye, X.W. Huang, J. Alloys Compd. 455 (2008) 420–423.
[23] B. Yan, C. Wang, J. Alloys Compd. 462 (2008) 147–152.
[24] I.G. Van Uitert, J. Electrochem. Soc. 114 (1967) 1048–1053.
[25] L. Ozawa, P.M. Jaffe, J. Electrochem. Soc. 118 (1971) 1678–1679.
[26] H.Y. Du, J.F. Sun, Z.G. Xia, J.Y. Sun, J. Electrochem. Soc. 156 (2009) J361–J366.